CrossMark

RESEARCH PAPER

Global representation of the drying–wetting curves of four engineering soils: experiments and correlations

Zhong-Sen Li[1,5] · Assia Benchouk[2] · Feth-Ellah Mounir Derfouf[2,6] ·
Nabil Abou-Bekr[2] · Said Taibi[3] · Hanène Souli[4] · Jean-Marie Fleureau[1]

Abstract The main objective of this paper is to examine how different engineering soils react to environmental variations and to provide correlations to characterize their behaviour under null external mechanical stress. Two French and two Algerian soils with liquid limits ranging from 36 to 112 were prepared under both slurry and Proctor compaction conditions, and then subjected to drying–wetting paths with suction controlled from several kPa to several hundreds of MPa. Experimental results are presented in five diagrams to show globally and simultaneously the shrinkage–swelling, saturation–desaturation and water retention characteristics. A reasonable consistency was observed between the oedometric and drying curves of slurry, confirming the equivalence between hydraulic loading (suction) and mechanical loading (consolidation stress) on the volume change behaviour of different soils. As an intrinsic parameter of soil nature, liquid limit was found to have a significant influence on the shrinkage limit, air-entry suction and compressibility of both slurry and compacted samples. For that reason, correlations between these characteristics and liquid limit were set up, providing a good basis for a first estimation of the drying–wetting curves. At the micro-scale, new experimental results were obtained: either on drying or wetting path, the micro-pores were almost unaffected, whereas, when matrix suction increased from 0.1 to 8 MPa, the volume of macro-pores decreased to quasi-closure. At last, the analogy between the compaction and drying–wetting curves, and the comparison of different methods to determine the water retention curve were addressed. Such analogies and comparisons contribute to a better understanding of the mechanisms of mechanical stress and suction.

Keywords Clay · Compaction · Drying–wetting curves · Effective stress · MIP · Suction

✉ Jean-Marie Fleureau
jean-marie.fleureau@centralesupelec.fr

1   Laboratoire de Mécanique des Sols, Structures et Matériaux - CNRS UMR8579, CentraleSupélec, Châtenay-Malabry, France

2   Laboratoire Eau et Ouvrages dans Leur Environnement, Université Abou-Bekr Belkaid, Tlemcen, Algeria

3   Laboratoire Ondes et Milieux complexes - CNRS UMR 6294, Université du Havre, Le Havre, France

4   Laboratoire de Tribologie et Dynamique des Systèmes - CNRS UMR 5513, Ecole Nationale d'Ingénieurs de Saint Etienne, Saint Étienne, France

5   School of Earth Science and Geological Engineering, Sun Yat-Sen University, Guangzhou, China

6   Department of Civil and Hydraulic Engineering, Dr Tahar Moulay University, Saïda, Algeria

List of symbols

C_{ms}	Swelling index with respect to void ratio
D_{ms}	Swelling index with respect to water content
e	Void ratio
e_{SPO}	Void ratio at standard Proctor optimum
G_s	Solid density
I_P	Plasticity index
m_s	Mass of solid
s	Suction
s_{AE}	Air-entry suction
s_{SL}	Shrinkage limit suction
s_{SPO}	Suction at standard Proctor optimum
S_r	Degree of saturation
T_{Hg}	Surface tension of mercury
T_w	Surface tension of water
w	Water content

w_L	Liquid limit
w_P	Plastic limit
w_{SPO}	Water content at standard Proctor optimum
w_{SL}	Water content at shrinkage limit
w_{AE}	Water content at air-entry
θ_w	Contact angle of water–solid phases
θ_{Hg}	Contact angle of mercury–solid phases
ρ_d	Dry density
$\rho_{d\text{-}SPO}$	Dry density at standard Proctor optimum
$\Delta w_{L\text{-}SL}$	Water content change from liquid limit to shrinkage limit
γ_s	Specific weight of grains
γ_w	Specific weight of water

1 Introduction

Engineering soils refer to the soils used in various engineering constructions. Compared to the soils usually used in research works (e.g. pure kaolinite, illite and montmorillonite), they contain several minerals and thus have relatively complex hydraulic and mechanical behaviours. Under natural conditions, engineering soils are inevitably subjected to drying–wetting paths due to the fluctuations of relative humidity caused by, for example, moisture changes under rainy and drought conditions. This phenomenon plays a major part in many problems affecting geotechnical structures, for instance, settlement or crack of foundations during drying, swelling or collapse of embankments during wetting, etc. In France, the damage caused by soil shrinkage was estimated to be more than 3.3 billion euro in 2002 [87] and this amount has been increasing as a result of frequently extreme climate. For safety and economic reasons, it is useful, necessary and urgent to investigate the mechanisms involved in drying–wetting paths and to put the knowledge into engineering practice.

In the absence of external mechanical stress, free drying or wetting leads to changes in soil volume, water content as well as degree of saturation, and the key driving parameter associated with these changes is suction. Starting from the water-saturated condition, as suction increases, soil gets desaturated as a result of water transfer from the porous medium to the environment, which, at the same time, results in volume change (shrinkage). On the contrary, in the case of an air-saturated sample, with the decrease in suction, water enters the soil, leading to an increase in degree of saturation and volume (swelling). The cyclic variations of volume, water content and degree of saturation on drying–wetting paths are of considerable importance in soil mechanics applied to shallow foundations and were investigated both experimentally and numerically over the last decades.

In the context of landslides prevention, earthwork construction and, more recently, radioactive waste disposal, drying–wetting tests were performed in order to relate the shrinkage–swelling or water retention behaviour to suction (e.g. [7, 29, 33, 35, 58, 72, 80, 82, 86]). The fruitful experimental data permitted the determination of compressibility (e.g. [84, 85]), permeability (e.g. [37, 81]) as well as shear strength (e.g. [15, 38]) of different engineering soils, in particular expansive clay and collapsible loess. Several parameters affecting drying–wetting curves such as temperature (e.g. [41, 51, 74]), stress history (e.g. [56, 59, 64]) and mineralogy (e.g. [40, 88]) were highlighted and well-illustrated thanks to recently developed techniques such as mercury intrusion porosimetry (MIP), scanning electron microscopy (SEM) and micro-computed tomography (μ-CT) (e.g. [24, 71, 73]). In this domain, another interesting aspect is the analogy between the effect of mechanical stress and that of suction in terms of volume change. By comparing the results of mechanical consolidation and drying tests, some authors [14, 18, 46, 53, 57, 86] found that the drying curve of saturated slurry was equivalent to an isotropic or oedometric consolidation curve, provided that suction was smaller than the air-entry value, i.e. the soil remained quasi-saturated. As explained by Taibi [76], at the micro-scale, the increase in suction on drying path induces the formation of water menisci between soil particles. When the sample is in quasi-saturated state, water fills all the voids, and the stress field applied to soil particles by surrounding water (equal to the value of suction) can be considered to be identical to that of isotropic or oedometric consolidation stress.

The above experimental results promoted the development of several models. At first, correlations between the soil intrinsic parameters (such as liquid limit, plasticity index and pore size distribution) and the soil volume change, as well as water retention behaviour, were established [11, 16, 33, 35, 42, 59, 60]. Then, several elastoplastic constitutive models were developed to predict with reasonable accuracy the volumetric deformations of unsaturated soils subjected to changes in stress and suction [6, 8, 48, 49, 61, 89]. However, most of these models are unable, in their present state, to calculate directly the corresponding changes in degree of saturation. In these models, the key parameters of the drying–wetting curves (e.g. air-entry suction, shrinkage limit) must be introduced. The knowledge of the drying–wetting curves is also required in semi-empirical models such as those proposed by [44, 55, 63].

The determination of drying–wetting curves is time-consuming and effort-requiring, so that it was, in most of the previous works, limited to the measurement of water content. The change in saturation with suction, however, was often not taken into account as it requires the

determination of both water content and void ratio of soil specimens under each applied suction, which is usually cumbersome. Besides, as drying–wetting curves are highly stress dependent, the large quantity of experimental results in the literature for different stress histories (e.g. slurry, statically or dynamically compacted, normally or over-consolidated samples) is virtually difficult to use directly for modelling.

For the above reasons, based on experimental works conducted at Ecole Centrale Paris in the past decades [14, 33, 35, 88], a comprehensive experimental plan was set up to investigate the drying–wetting curves of four engineering soils prepared under both slurry and Proctor compacted conditions. The experimental results together with those reported in the literature for the same stress history conditions contribute: (1) to globally understand the drying–wetting curves and the effect of influencing factors (e.g. soil nature, initial water content, stress history); (2) to make a comprehensive analogy between hydraulic and mechanical loadings, for example, through the comparison between compaction and drying–wetting curves, the analogy between the effect of mechanical stress and suction on soil volume change behaviour, etc.; and (3) to correlate the main parameters of drying–wetting curves with liquid limit. In addition to bring out relatively comprehensive and systematic experimental data to the researchers for further numerical modelling and to the practicing engineers for a first estimation of the soil behaviour, the novelties of the paper are:

- To show the drying–wetting paths in a global way and present compaction curves with matrix suction as well as iso-suction lines;
- To provide new experimental proof about the suction effect on the micro-structure change of compacted clay;
- To confirm with new experimental results the validity of the Terzaghi effective stress approach in quasi-saturated domain (i.e. when the applied suction is smaller than the air-entry suction).

The paper follows the following structure: Sect. 1 introduces the background and main contributions of the present work, and paves the way for Sect. 2 that describes in details the global representation of drying–wetting curves; as routine parts, Sects. 3 and 4 introduce the experimental materials and methods, respectively. In Sect. 5, the experimental results on drying–wetting curves of four soils under slurry and Proctor compacted conditions are presented; by taking advantage of the data in this study and others available in the literature, Sect. 6 tries to correlate some important parameters of drying–wetting curves with liquid limit, and Sect. 7 is dedicated to illustrating and comparing the mechanisms of hydraulic and mechanical loadings; at last, Sect. 8 lists the main conclusions.

2 Global representation of drying–wetting curves under nil external mechanical stress

The first half of the twentieth century witnessed the expansion of interest in research about the relationship between water content and suction. Impressive studies, carried out by soil scientists (e.g. [20, 39, 66–68]), set up a fundamental basis for the subsequent investigation of drying–wetting curves in geotechnical engineering (e.g. [16, 26, 27]). In the late 1980s, the representation of drying–wetting curves was extended and developed into five diagrams that describe globally and simultaneously the shrinkage–swelling, variation of saturation and water retention behaviour of soils (e.g. [14, 45]). As shown in Fig. 1, the global presentation of drying–wetting curves consists of:

- the shrinkage–swelling curves (Fig. 1a, b): in the upper left $[w, e]$ diagram, as a measure of volume change, void ratio is plotted against water content. On the drying curve, the soil first follows the saturation line with the equation $e = \gamma_s/\gamma_w \times w$. Then, as water content continues to decrease, void ratio tends towards a constant value. The shrinkage limit w_{SL} is defined as the intersection between the saturation line and the horizontal asymptote of the dying or wetting curve when w tends to zero. In the upper right $[s, e]$ diagram, void ratio is plotted against suction, showing the compressibility under hydraulic loading. The drying curve shows two distinct phases: a first phase which is similar to the compression of a saturated soil, as evidenced by the parallelism between the drying curve and the oedometric or isotropic compression curves; a second phase where the soil becomes quasi-rigid and behaves elastically. The transition suction between the two domains, s_{SL}, is termed "shrinkage limit suction" and plays an important role in modelling [50, 61].
- the saturation–desaturation curves (Fig. 1c, d): the middle left $[w, S_r]$ diagram presents the change in degree of saturation with water content. At the beginning of the drying path, the degree of saturation changes insignificantly up to a point beyond which it decreases almost linearly with water content. This point, termed "air-entry point", is defined as the intersection of the two asymptotic lines. The middle right $[s, S_r]$ diagram shows the change in degree of saturation with suction. Corresponding to the air-entry value, the air-entry suction, s_{AE}, is defined as the intersection of the asymptotic lines.
- the water retention curve (WRC) (Fig. 1e): the last $[s, w]$ diagram shows the capacity of gravity water to be absorbed by soil at different suctions and the water retention characteristics of the soil subjected to drying and wetting.
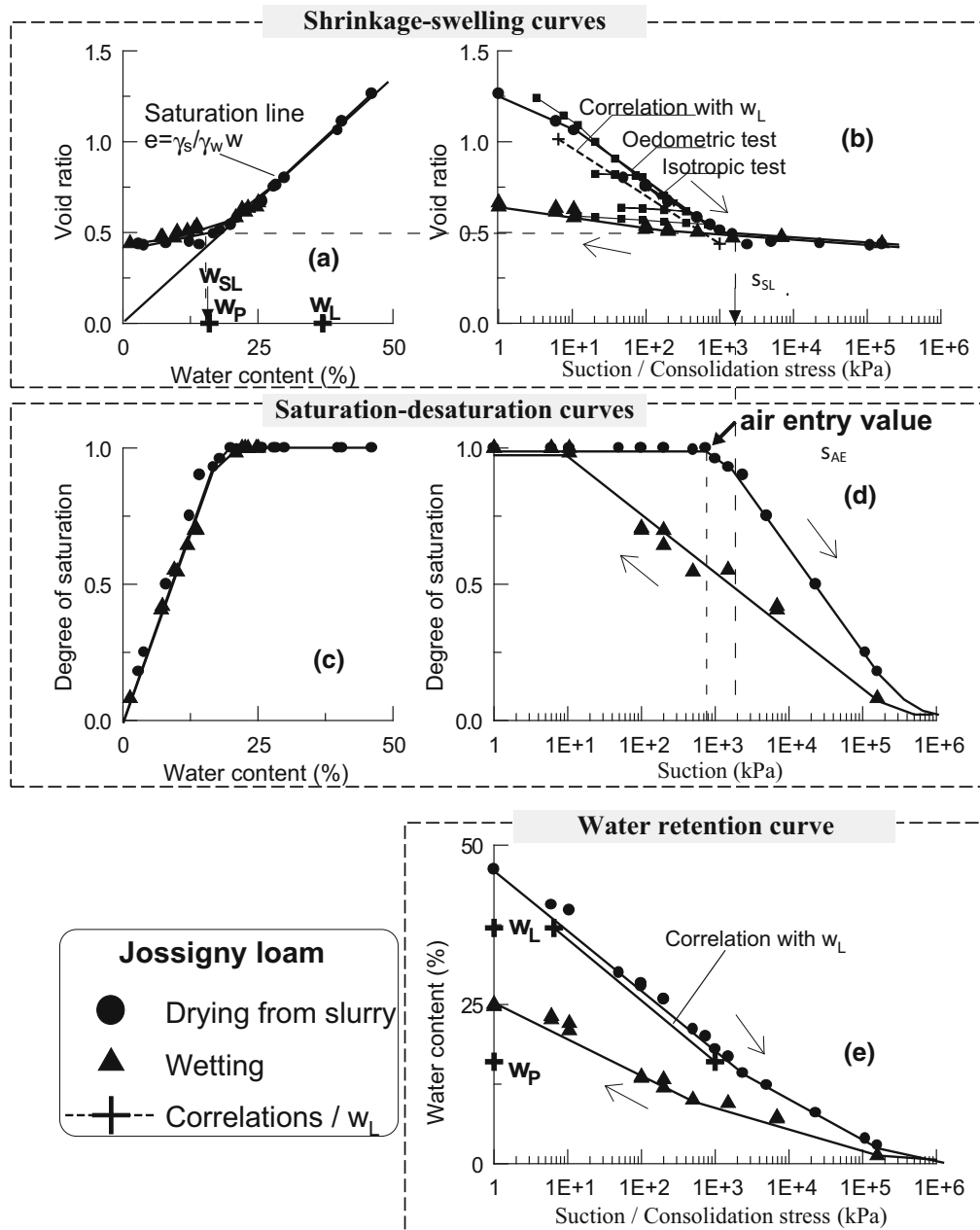
Fig. 1 Global representation of drying–wetting curves for the saturated slurry of Jossigny silt (after Fleureau et al. [33])

3 Materials

Two engineering soils from France (Camargue silt, Châtaignier clay) and two others from Algeria (Sikkak and Maghnia clays) were investigated in this research. Camargue silt is a core material currently used in the Rhône dikes of Camargue area in the south of France. It is very heterogeneous, consisting of both clay and silt particles. Châtaignier clay is a subgrade material extracted from a site (Châtaignier village) near the Tours–Bordeaux high-speed railway line in the south-west of France. It contains

mainly clayey particles with large specific surface area, but also some sharp gravel with diameters of several centimetres, which were eliminated manually before the laboratory tests. Sikkak and Maghnia clays are local materials from the areas of Sikkak and Maghnia, 20 km north and 60 km north-west of the Tlemcen city, respectively, in the west of Algeria. Sikkak material was used in the core of an earth dam, and Maghnia clay is a bentonite deposit.

The grain size distribution and the main geotechnical properties of the four materials are shown in Fig. 2 and Table 1, respectively.

4 Methods

The materials taken from the different sites were first dried under laboratory conditions (20 ± 1 °C) for more than 3 weeks, then crushed with a rubber mallet and finally sieved at 2 mm. The passing particles were dried in an oven at 105 °C for about 2 days and mixed afterwards with the required quantity of distilled water to prepare the saturated slurry or compacted samples.

To prepare the saturated slurry, a quantity of distilled water corresponding to 1.5 times the liquid limit was mixed with 2 kg dried soil particles. In order to get rid of the air bubbles, the mixed slurry was stirred carefully by a mechanical agitator for more than 2 days. Oedometric and isotropic compression tests were performed on the prepared slurry.
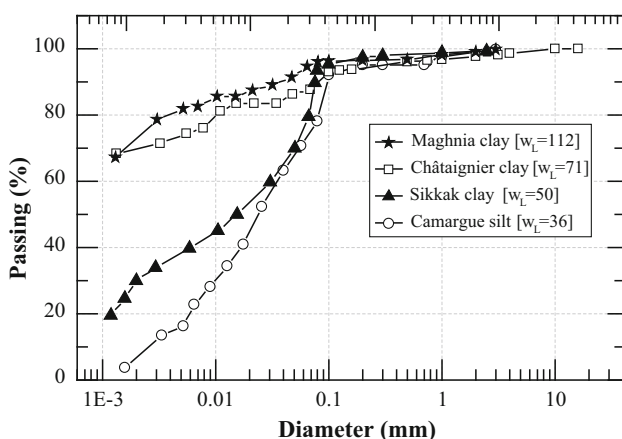

Fig. 2 Grain size distribution of the soils studied in this research

Concerning the preparation of compacted samples, the moist Camargue, Sikkak and Maghnia soils were compacted under Proctor conditions in a mould, 11.6 cm high and 10.1 cm in diameter, in three layers, each layer receiving 25 blows from a 2.490 kg rammer dropping from a height of 30.5 cm. For comparison purposes, the Châtaignier clay was compacted with 15, 25 and 35 blows per layer, called reduced Proctor (RP), standard Proctor (SP) and enhanced Proctor (EP), corresponding to specific energies of 0.36, 0.60 and 0.84 MJ/m^3, respectively.

During the Proctor test, suction was measured by means of filter-paper and thermocouple psychrometers. For the filter-paper method, the Whatman 42 filter-paper was cut into small pieces of 6 cm in diameter and then sandwiched into two ordinary filter-papers of 8 cm in diameter. The sandwiched filter-paper was carefully laid on each compacted layer, covered with the same soil and compacted again. The whole compacted sample was thereafter put in a plastic bag and sealed with a rubber ring. After 2 weeks, the filter-paper was taken out and its water content was measured quickly (within 5 s) by an analytical balance, with a precision of 0.001 g. The corresponding suctions in the first and second layers were back-calculated using the calibration curves of Chandler et al. [23]. For the thermocouple psychrometer method, the Wescor Dew Point Microvoltmeter (model HR-33T) was used to determine soil suction in the compacted Châtaignier clay. A calibrated ceramic transducer (model PCT-55) was buried into the compacted sample. After 2 days, equilibrium was reached and soil suction was calculated by comparing the measured relative humidity with that of calibration by

Table 1 Main geotechnical properties of the materials and the corresponding correlations from the literature (SPO: standard Proctor optimum)

	Camargue silt	Châtaignier clay	Sikkak clay	Maghnia clay	Standards
G_s	2.70	2.83	2.64	2.72	NF P94-054 [1]
Grain size distribution (%)					NF P94-057/056 [2, 3]
<80 mm	72	88	78	82	
<2 μm	42	70	45	48	
Atterberg limits (%)					NF P94-051 [4]
w_L	36	71	50	112	
w_P	24	37	23	45	
I_P	12	34	27	67	
w_{SPO} (%)					NF P94-093 [5]
Measured	17.2	37.5	16	18	
Fleureau et al. [35][a]	17.0	28.6	22.0	38.5	
$(\gamma_d/\gamma_w)_{SPO}$ (kN/m^3)					
Measured	17.2	13.1	15.5	12.3	
Fleureau et al. [35][b]	17.2	14.2	15.9	11.4	

[a] $w_{SPO} = 1.99 + 0.46w_L - 0.0012w_L^2$

[b] $(\gamma_d/\gamma_w)_{SPO} = 21.00 - 0.113w_L + 0.00024w_L^2$

NaCl solution. It must be noted that filter-paper measures the matrix suction while psychrometer measures total suction. More details about the filter-paper and thermocouple psychrometer methods can be found in the works of Bulut et al. [21] and Verbrugge [84, 85], respectively.

When the above steps were performed, the compacted sample was carefully cut into small bricks of 2–3 cm^3, with smooth surfaces. Then, the small specimens, slurry or compacted, were put into different devices for drying–wetting tests.

Four methods, namely tensiometric plate, osmotic, desiccator and dynamic vapour sorption (DVS) methods, were used to control soil suction. Tensiometric plate controls suction between a few kPa and 20 kPa. It consists of a sintered glass with low porosity that serves as a semipermeable filter, set in a glass funnel. Soil sample is placed on the sintered glass in contact with a reservoir filled with de-aired water and connected to a horizontal measurement tube. When the measurement tube is placed lower than the reservoir, it imposes a negative pressure (i.e. a pressure lower than the atmospheric) to the water in the reservoir. To produce suctions in the range from 100 to 8000 kPa, the osmotic method was used. The sample is placed on a dialysis membrane, which is tightly sealed by two clamps, and then put into the polyethylene glycol (PEG) 20,000 solution until equilibrium (2 weeks). The value of suction depends on the concentration of PEG. For higher values of suction, the method consists in putting the sample in an atmosphere with a given relative humidity. This is achieved either with saturated salt solutions or a dynamic vapour sorption (DVS) device. When a saturated salt is in thermodynamic equilibrium with its vapour, the relative humidity of the surrounding atmosphere remains constant at a given temperature. The relative humidity depends on the nature of the chemical salt. The DVS device is a vapour generator with precise control of relative humidity and temperature that allows measuring the resulting weight of the sample. It must be noted that, for the methods described above, both tensiometric plate and osmotic technique control matrix suction, whereas the desiccator and DVS techniques control the total suction in soil samples. Details of the tensiometric plate method are given by ASTM D 6836-02 [10] and Vanapalli et al. [83]; the osmotic method is described by Blatz et al. [17], and Fleureau and Kheirbek-Saoud [34]; the desiccator and DVS technique are referred to the work of Coronado et al. [25] and Li [53].

In addition to the above methods, the suction effect on compacted clay was studied at the micro-scale by performing mercury intrusion porosimetry (MIP) tests on compacted Châtaignier clay samples that had been subjected to different suctions. The method, which consists mainly of freeze-drying and mercury intrusion steps, is described and analysed in Delage et al. [31].

5 Experimental results

This section includes four subsections, which introduce successively the results of: (1) Proctor compaction test on Châtaignier clay; (2) drying–wetting tests on Camargue silt as well as Châtaignier, Sikkak and Maghnia clays prepared under saturated slurry condition; (3) drying–wetting tests for the above four materials compacted with standard Proctor compaction energy; (4) drying–wetting tests on Châtaignier clay compacted under different conditions. In addition, results of suction effect on the macro- and micropores of Châtaignier clay are also presented.

5.1 Compaction curves

Figure 3 presents the compaction curves and the contours of equal suction for the Châtaignier clay. As compaction energy increases from 0.36 (RP) to 0.84 MJ/m^3 (EP), the optimum water content decreases from 40 to 33.5%, while the corresponding dry density increases from 1.26 to
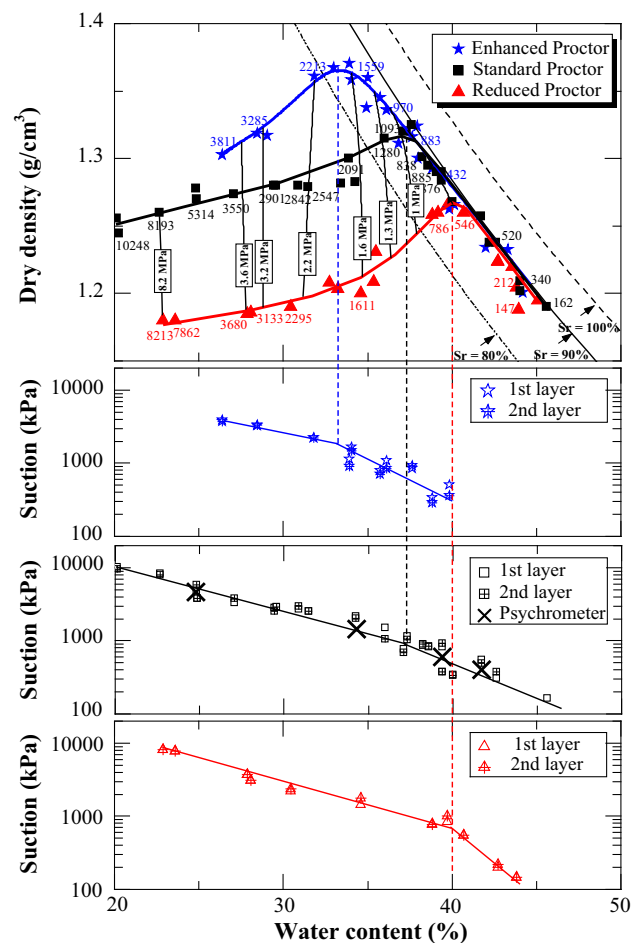
Fig. 3 Compaction curves and change in suction with water content at reduced, standard and enhanced Proctor conditions (Châtaignier clay)
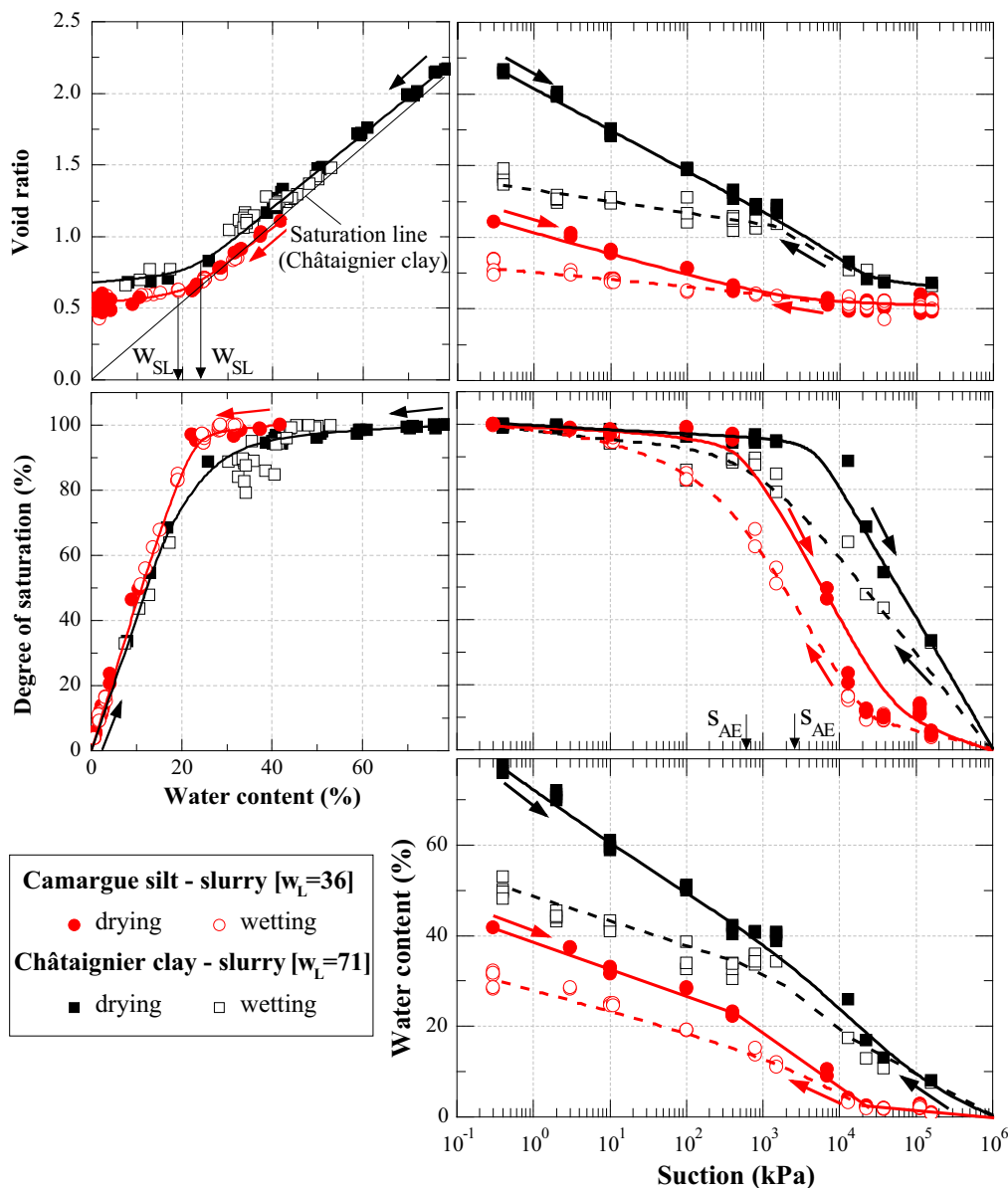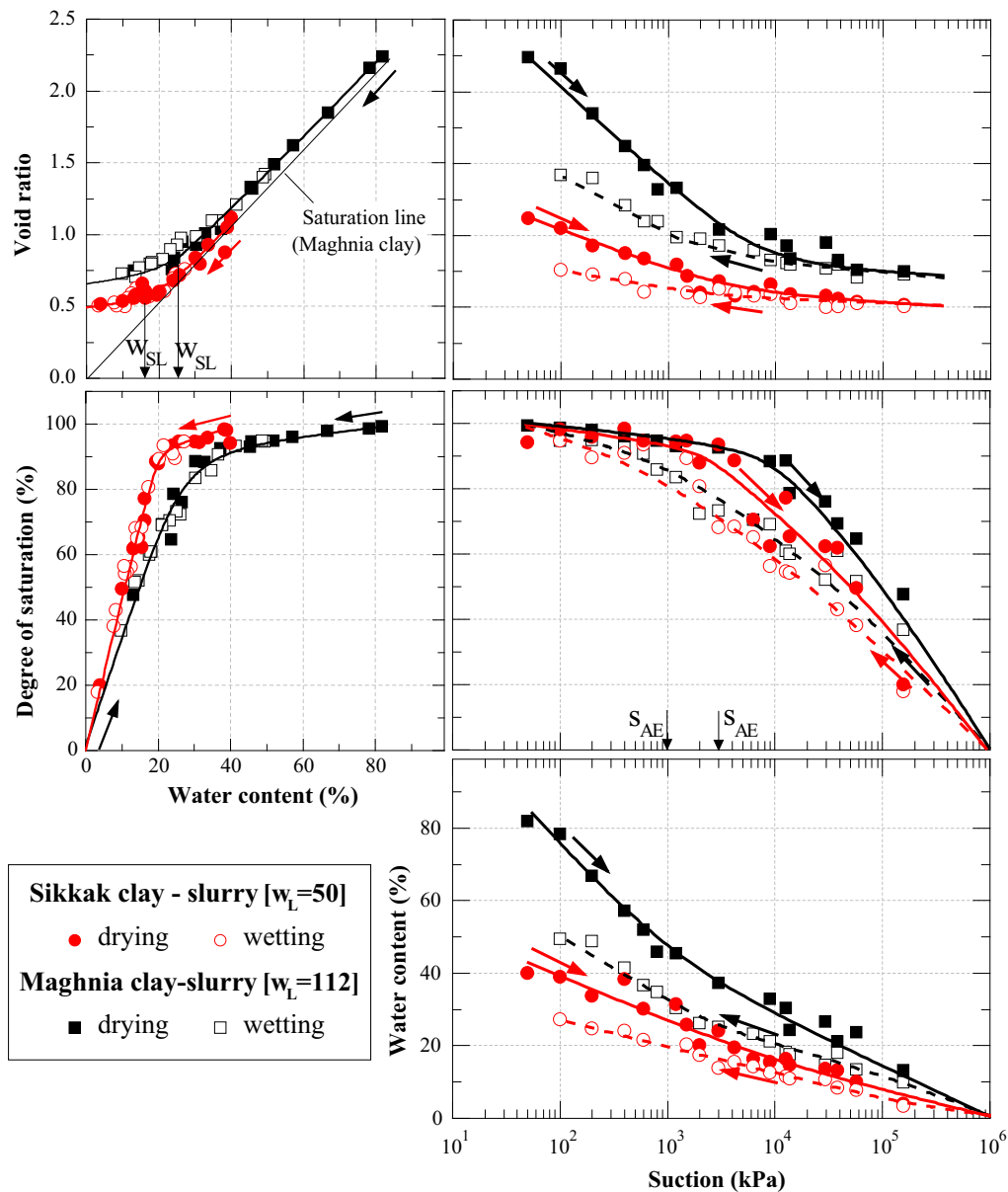
Fig. 4 Drying–wetting curves of saturated slurries of Camargue silt and Châtaignier clay (for drying paths, samples were prepared at $w_i = 1.5w_L$; for wetting path, samples were prepared at $w_i = 1.5w_L$, then dried in an oven)

1.37 g/cm^3. As already observed by several authors, higher compaction energy is accompanied by higher maximum dry density and lower optimum water content. On the dry side of the optimum (e.g. $w < 30\%$), the contours of equal suction are almost vertical, showing that suction is independent of dry density whereas, on the wet side, the contours of matrix suction become progressively parallel to the saturation line. Similar results were reported for different soils such as Chinese loess [52], Boom clay [70] and Speswhite kaolin [78]. These results illustrate that, for clayey soils, matrix suction is mainly determined by the absorbed water in the intra-aggregate voids: on the dry side, compaction stress compresses inter-aggregate voids

that do not contain (or contain very little) free water, and intra-aggregate voids are almost not compressed, so that suction is not influenced; by contrast, on the wet side, as the degree of saturation increases, loading mechanism begins to affect the intra-aggregate voids, resulting in lower measured matrix suctions.

Figure 3 also presents the relationship between suction and water content. In a semi-logarithmic coordinate system, matrix suction is observed to be a linear function of water content on both sides of the optimum. The absolute value of the slope on the wet side of the optimum appears to be larger than that on the dry side, resulting from the different fabrics of compacted soils on the dry and wet

Fig. 5 Drying–wetting curves of saturated slurries of Sikkak and Maghnia clays (for drying paths, samples were prepared at $w_i = 1.5w_L$; for wetting path, samples were prepared at $w_i = 1.5w_L$ and then dried in an oven)

sides. Similar results were reported by Marinho and Stuermer [58], Fleureau et al. [35] and Taibi et al. [77] for several soils in a relatively large range of liquid limits.

5.2 Drying–wetting curves of saturated slurries

Figures 4 and 5 present the drying–wetting curves of the four soils prepared as slurries. The global representation highlights the difference in soil volumetric and saturation behaviours with respect to water content and suction: in the (w, e) and (w, S_r) planes, the drying and wetting curves approximately coincide with each other; however, in the (s, e), (s, S_r) and (s, w) planes, an apparent hysteresis is

observed. Such observations illustrate that hysteresis is apparent in the plane of void ratio or saturation versus suction, and it almost disappears when plotting the parameters against water content. Besides, the experimental results show the significant influence of liquid limit on the characteristics of drying–wetting curves: when liquid limit increases from 36 to 112, shrinkage limit increases from 19 to 24%, and the air-entry suction goes up, from 600 to 3000 kPa.

In order to show the analogy between the effect of suction and that of mechanical stress, the oedometric curve was compared with the drying curve in the same diagram (Fig. 6). The results show that: for Camargue, Sikkak and
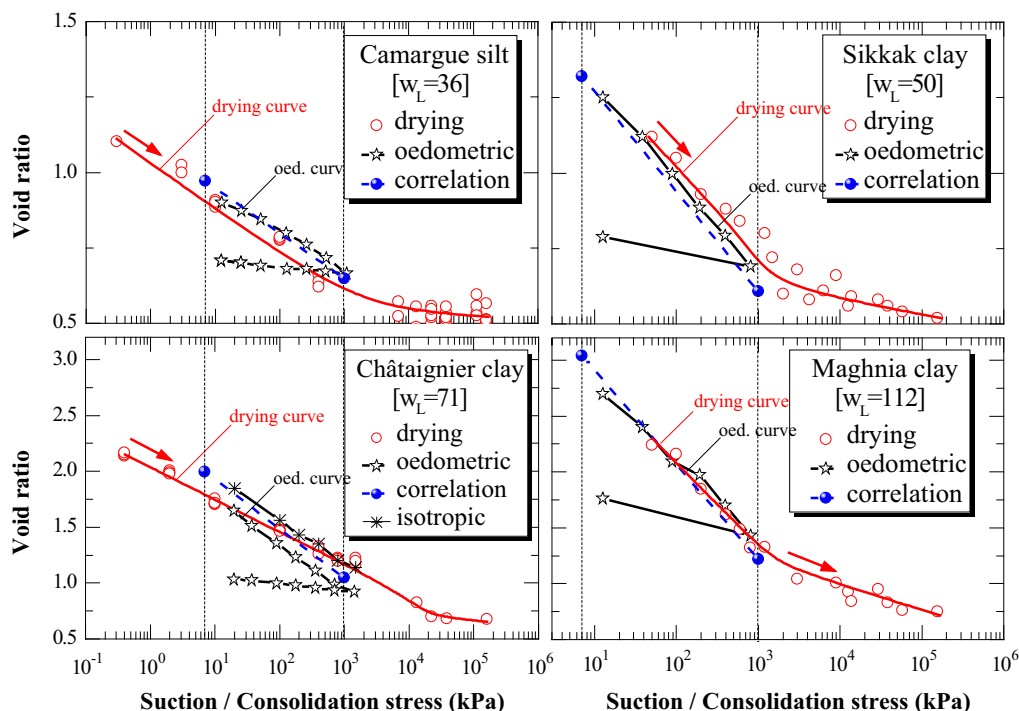
Fig. 6 Comparison of drying curves with oedometric or isotropic compression curves, and with the empirical correlation proposed by Biarez and Favre [13]

Maghnia materials, the drying curve is very close to the oedometric curve; however, for Châtaignier clay, the slope of the drying curve was found to be a bit smaller than that of the oedometric curve—such difference may come from the effect of the semi-permeable membranes in both tensiometric plate and osmotic techniques.

In the work of Biarez and Favre [13], the authors found that isotropic consolidation curve can be characterized by the following reference lines:

$$w = w_L \text{ or } e = G_s \times w_L \text{ for } s = 7\,\text{kPa} \tag{1}$$

$$w = w_P \text{ or } e = G_s \times w_P \text{ for } s = 1000\,\text{kPa} \tag{2}$$

For comparison purpose, the above reference lines were plotted and show satisfactory ability to predict both oedometric and drying curves for Camargue, Sikkak and Maghnia materials.
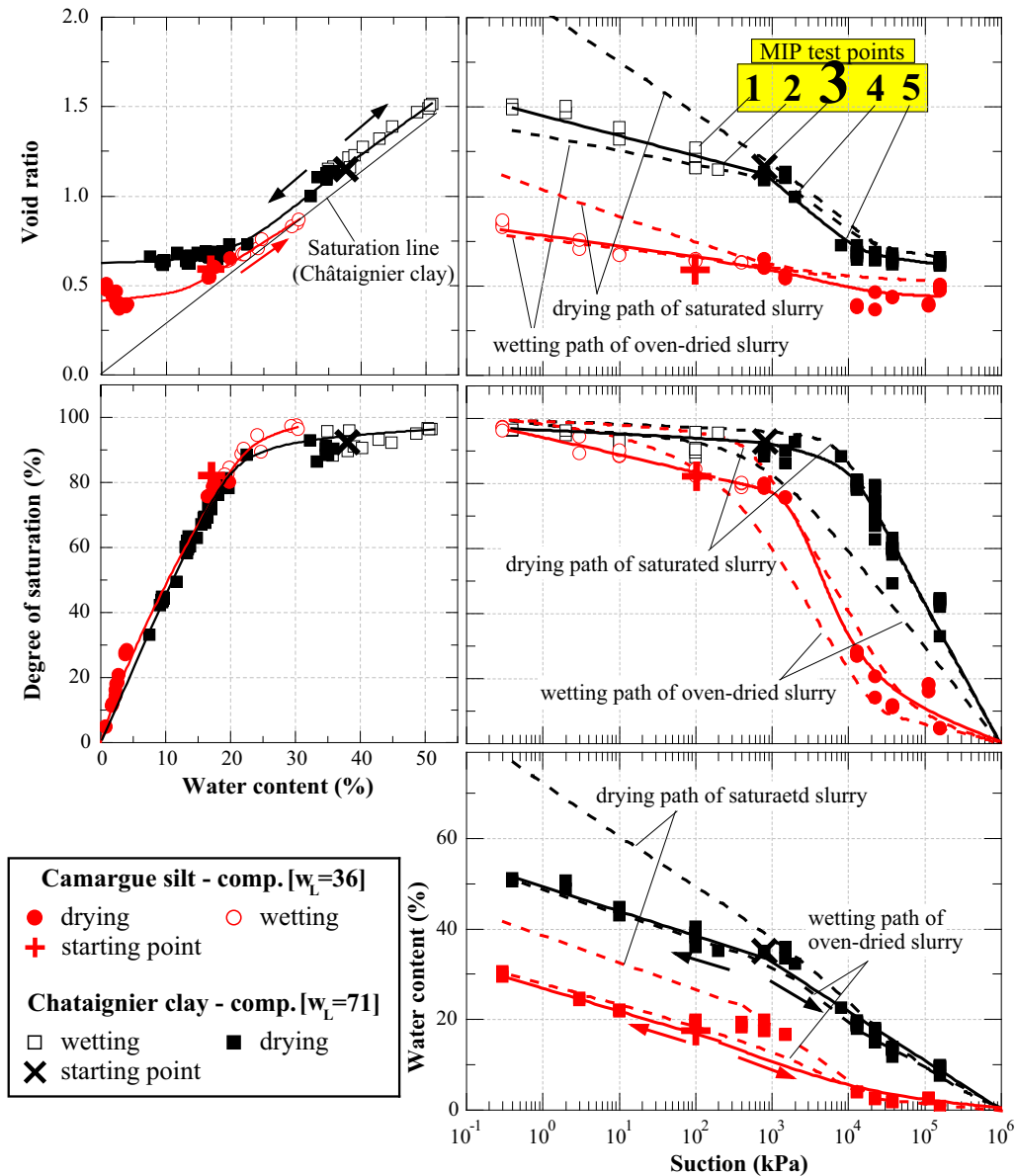
5.3 Drying–wetting curves of standard Proctor compacted samples

Figures 7 and 8 present the drying–wetting curves under standard Proctor compaction conditions. For comparison purpose, the corresponding drying–wetting curves of saturated slurry were plotted using dashed lines.

Concerning the volume change behaviour, starting from the optimum point, the samples subjected to suctions larger than the initial one experience shrinkage, those subjected to

suctions lower than the initial one experience swelling. In the (s, e) plane, the wetting curve is approximately linear, similar to those reported in the literature [35, 41, 77, 82]. For the two French soils, the slope of the wetting curve is smaller than that of the drying curve, showing that compressibility under suction loading (drying) is larger than that under suction unloading (wetting). Such results are similar to those of oedometric tests, where compressibility under mechanical loading is generally larger than that during unloading. However, for the two Algerian soils, the results are opposite, probably due to the presence of montmorillonite in the two clays, which generally exhibits a large expansibility during wetting. In the study, the wetting curve of the compacted sample is superposed to that of the oven-dried slurry. Even so, one should be careful about this similarity as the microstructures of the Proctor compacted soil and oven-dried slurry are quite different: compacted samples generally show a bimodal pore structure while oven-dried slurry samples usually feature unimodal pore structure.

In addition to the above shrinkage–swelling curves, the MIP tests provide a micro-approach to investigate the variation of the pore size distribution during drying and wetting. As shown in Fig. 9, on the wetting path, water moves into the compacted sample and creates more interaggregate pores, so that the volume of major inter-aggregate pores increases; on the other hand, on the drying path, as suction increases, water flows out of compacted samples

Fig. 7 Drying–wetting curves of compacted samples under standard Proctor optimum conditions (w_{SPO} = 17.2% for Camargue silt; w_{SPO} = 37.5% for Châtaignier clay) and comparison with those prepared under saturated slurry conditions

and the major inter-aggregate pore volume decreases. Besides, it is interesting to note that the major inter-aggregate pores become closed at suctions as high as 8 MPa, which is consistent with the macroscopic behaviour in which the shrinkage limit suction is also about 8 MPa. For the studied material and the applied suction, the major intra-aggregate pores with a diameter of about 20 nm were almost unchanged. The above results confirm the observation of Alonso et al. [9] that, for non-active clay, suction and stress applied to compacted specimens modify mainly the macro-porosity.

As regards the water retention behaviour, in the (s, w) plane, again, the wetting curve of compacted samples is

very close to that of dried slurry. Similar to the suction change with respect to water content of the compacted path (Fig. 3), the drying and wetting curves can be represented by two linear lines in a semi-logarithmic plane. The absolute value of the slope, termed water capacity, reflecting the ability of the soil to absorb water, was used in various numerical correlations [35, 59, 60] to predict the water retention curve.

5.4 Drying–wetting curves of samples compacted at different energies and water contents

Figure 10 compares the drying–wetting curves of the Châtaignier clay compacted at three different water
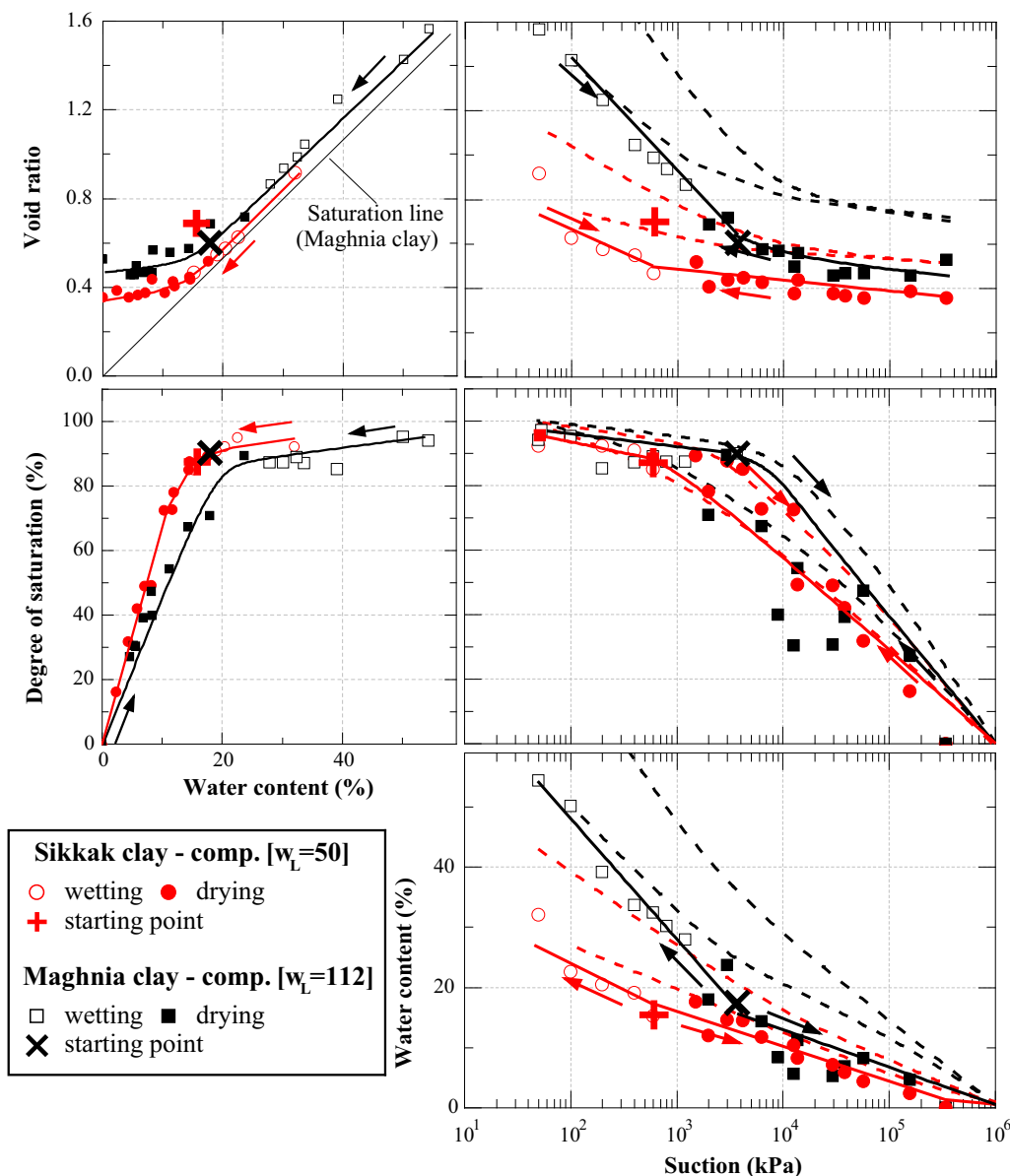
Fig. 8 Drying–wetting curves of compacted samples under standard Proctor optimum conditions ($w_{SPO} = 16\%$ for Sikkak clay; $w_{SPO} = 18\%$ for Maghnia clay) and comparison with those prepared under slurry conditions

contents: $w_{SPO} - 5$, w_{SPO} and $w_{SPO} + 5$. In general, the drying–wetting curves of the optimum condition lie between those prepared on the dry and wet sides of the optimum, as shown in the (s, e), (s, S_r) and (s, w) planes. For the sample compacted at $w_{SPO} - 5$, the air-entry suction is smaller than those at $w_{SPO} + 5$ and w_{SPO}. This can be inferred from the different micro-structures of the compacted samples: compared to the samples compacted at $w_{SPO} + 5$ and w_{SPO}. Samples at $w_{SPO} - 5$ usually exhibit larger major inter-aggregate pores, which is consistent with the lower air-entry suction. However, as regards the volume change and water retention behaviours, the results of this study, together with those presented by Fleureau et al.

[35], Marinho [57] and Marinho and Stuermer [58], show that the effect of the initial water content is negligible for compacted clays.

Figure 11 shows the drying–wetting curves of the samples prepared at different compaction energies. Many experiments (e.g. [35, 58]) showed the influence of compaction energy on drying–wetting curves and in particular the air-entry suction. This is not obvious in this study for the reasons that: (1) the applied energies (0.36, 0.6 and 0.84 MJ/m³) are not distinct enough to observe a clear difference; (2) dispersion of experimental results comes from the difficulty of the volume measurement. However, from the results, one can at least conclude that the compaction energy (in the
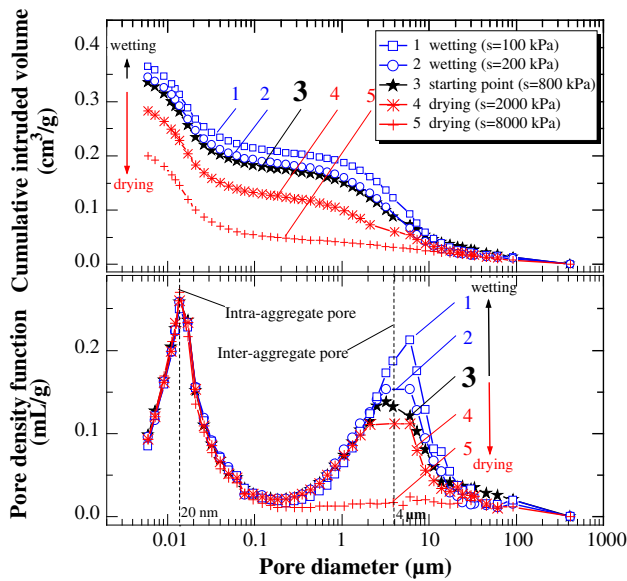
Fig. 9 Variation of the pore size distributions for the compacted Châtaignier clay after drying–wetting paths

tested range) has a limited influence on drying–wetting curves for the tested clayey soils.

6 Correlation

Historically, liquid limit (w_L) was deemed to be a suitable intrinsic parameter to represent the nature of soil (e.g. [22, 33, 35, 79]). From an engineering point of view, such representation provides an effective way to correlate the main geotechnical properties with soil nature. In this regard, liquid limit was chosen, in this study, as the basic parameter to characterize the main properties of the drying–wetting curves.

6.1 Correlations of air-entry suction and variation of water content with liquid limit for saturated slurries

In order to highlight the effect of soil nature on drying–wetting curves, the four soils described in this study, together with 17 other soils from the literature (Table 2), were considered and their characteristics were analysed. Correlations have been established between the air-entry suction (s_{AE}) and variation of the water content ($\Delta w_{L\text{-}SL}$) with liquid limit (Fig. 12):

$$s_{AE}(kPa) = -0.1w_L^2 + 50w_L - 1026(R^2 = 0.89) \quad (3)$$

$$\Delta w_{L-SL} = 0.9w_L - 16(R^2 = 0.96) \quad (4)$$

with $\Delta w_{L\text{-}SL}$, the change in water content from liquid limit (w_L) to shrinkage limit (w_{SL}): $\Delta w_{L\text{-}SL} = w_L - w_{SL}$; R, the regression coefficient.

6.2 Correlation of the wetting path for the standard Proctor compacted soils

As shown in Table 3, a total of 50 soils were analysed for the modelling of the wetting path. Figure 13 provides the correlations between the swelling index and liquid limit:

$$C_{ms} = 0.000026w_L^2 - 0.0018w_L + 0.039(R^2 = 0.92) \quad (5)$$

$$D_{ms} = 0.0009w_L^2 - 0.058w_L + 0.46(R^2 = 0.86) \quad (6)$$

with C_{ms}, swelling index with respect to void ratio; D_{ms} swelling index with respect to water content.

In addition, with this relatively large quantity of experimental data, it is also possible to correlate the properties of soils at standard Proctor optimum (SPO) with liquid limit:

$$w_{SPO}(\%) = 0.37w_L + 3.1(R^2 = 0.92) \quad (7)$$

$$s_{SPO}(kPa) = 23.4w_L - 512(R^2 = 0.95) \quad (8)$$

$$\rho_{d-SPO}(g/cm^3) = 0.000038w_L^2 - 0.013w_L + 2.17(R^2 = 0.90) \quad (9)$$

where w_{SPO}, s_{SPO} and $\rho_{d\text{-}SPO}$ represent the water content, suction and dry density at standard Proctor optimum, respectively.

7 Discussion

In this section, the effects of mechanical stress and suction are compared in terms of volume change for saturated slurry; hence, analogy between compaction curve and drying–wetting curves will be examined, and at last, the results of different ways of measuring and controlling suction will be synthesized and evaluated.

7.1 Comparison of the mechanical stress and suction for the saturated slurry

As previously observed by several researchers (e.g. 14, 18, 46, 52, 56), when the applied suction was smaller than the air-entry suction, drying curve presented in the [log(s), e] coordinate system was in fact very close to the oedometric or isotropic curve in the [log(p), e] coordinate system. Such observation is important as it reflects that suction and mechanical stress may have the same effect on the volume change behaviour if the soil is quasi-saturated. Further inspection of these previous results shows that the Terzaghi effective stress initially proposed for saturated soil ($s = 0$) is still valid for unsaturated soil ($0 < s < s_{air}$). From a theoretical point of view, these observations and inferences are reasonable as the water menisci formed in the sample can result in a real attractive force between particles, which
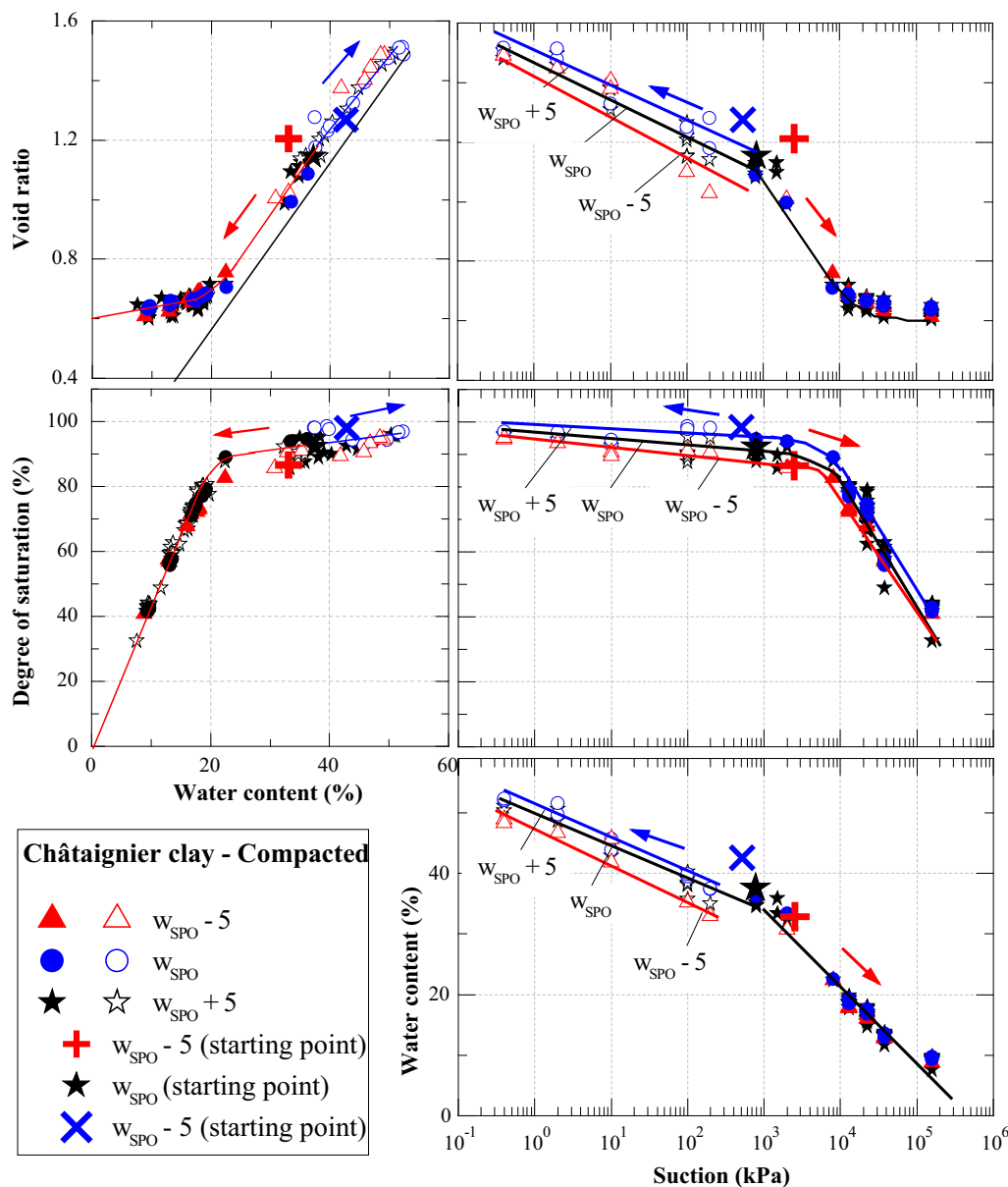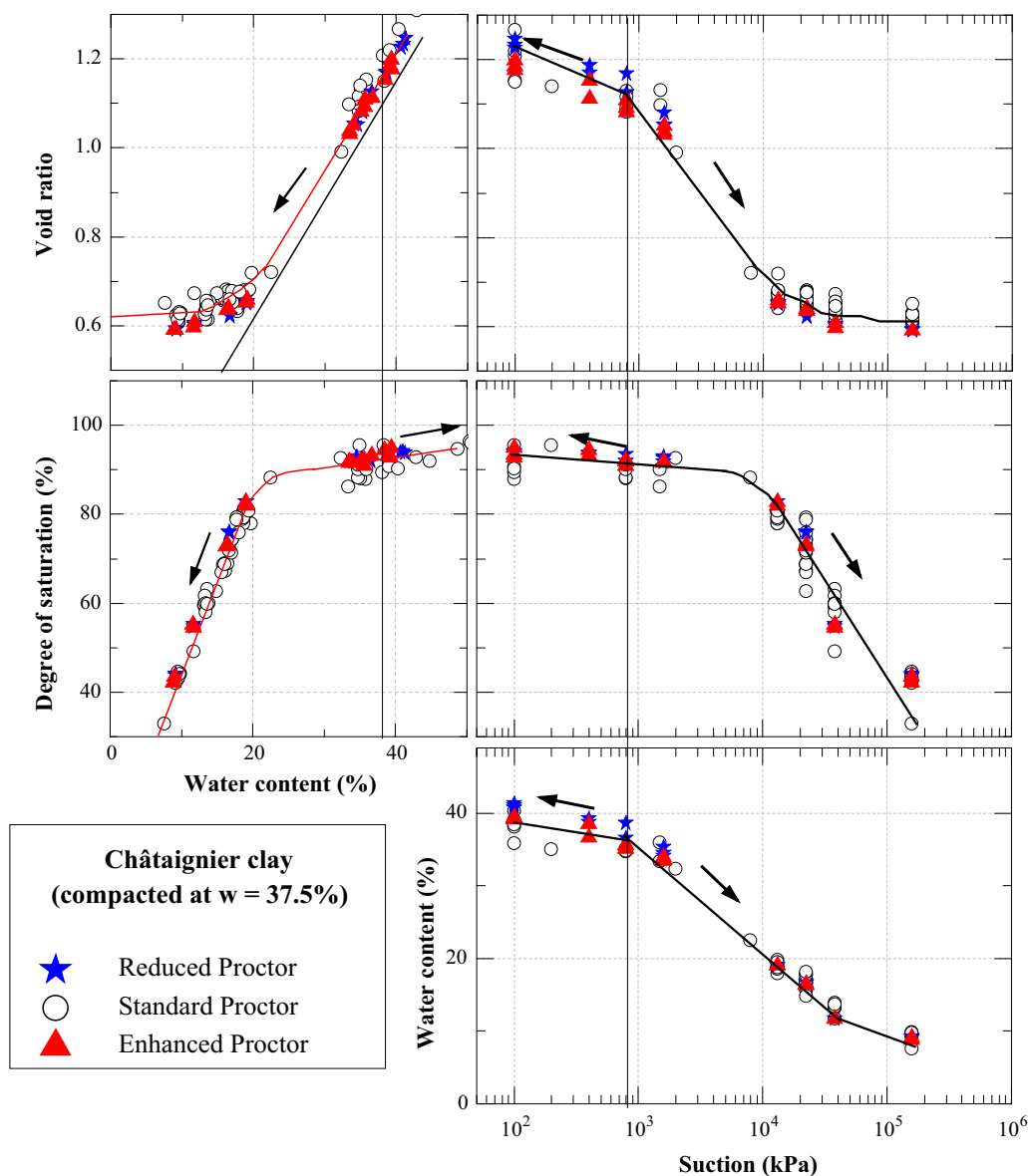
Fig. 10 Drying–wetting curves of the Châtaignier clay compacted at water contents of 32.5% ($w_{SPO} - 5$), 37.5% (w_{SPO}) and 42.5% ($w_{SPO} + 5$) with standard Proctor energy

should have the same effect as that induced by external mechanical loading.

Even though with some deviations for Châtaignier clay, the experimental results in Fig. 6 provide rigorous proof to confirm the above observation from the literature and the theoretical explanation about the equivalent effect of suction and mechanical stress on volume change behaviour. In the figure, both suction and consolidation stress lead to the volumetric change of samples, and if the difference resulting from the effect of semi-permeable membrane is neglected, the drying curve (caused by suction increase) can be considered to be equal to the oedometric or isotropic curve, which is in fact as a result of mechanical stress.

In addition, the empirical correlation line of Biarez and Favre [13], which was initially developed to predict the isotropic curve, is able to characterize, in a concise way, the drying curve in the [log(s), e] plane. In order to further examine the possibility of directly using this empirical method to predict drying curve, the experimental data of the four soils used this study and other 7 soils from the work of Fleureau et al. [33] were collected and then conjunctively presented in Fig. 14. From the figure, the isotropic correlation lines (dashed line) determined according to Eqs. (1) and (2) are reasonably consistent with experimental drying curves of various soils with liquid limit ranges from 27 to 160. Such observation confirmed that,

Fig. 11 Drying–wetting curves of Châtaignier clay compacted with reduced, standard and enhanced Proctor energies at 37.5% water content

for a first estimation, the drying curve can be reasonably represented by the correlations line of Biarez and Favre [13].

Based on Figs. 6 and 14, one can conclude that, for the saturated or quasi-saturated soil, the mechanical stress has an equivalent effect as suction in terms of volume change and Terzaghi effective stress is still valid; for a first estimation of the drying curve, the correlation line of Biarez and Favre [13] can be used.

### 7.2 Analogy between compaction curve and drying–wetting curves

In the literature, the comparison between compaction and drying–wetting curves has not been much addressed. In the

work of Fleureau et al. [35], however, the authors observed the possibility to derive the wetting curves of four soils from compaction tests in which suction was measured. Even though starting from different initial point and following very different processes (either hydraulic or mechanical), it is interesting to note, in the (w, s) plane, the similarity between compaction curve and wetting curve for Proctor compacted samples. In this study, the interest of further comparing the drying–wetting curves with compaction curve lies in examining whether the above correspondence exists or not in other planes [e.g. (w, S_r), (s, S_r)], for different soils and under different compaction conditions.

With the compaction curve in Fig. 3, it is possible to present the compaction curve in a more comprehensive way with the following calculations:

Table 2 Materials used for the correlation of air-entry suction (s_{AE}) and variation of water content ($w_L - w_{SL}$) under saturated condition ($w_i = 1.5w_L$)

Material no.	Soil	w_L (%)	s_{AE} (kPa)	w_{SL} (%)	$w_L - w_{SL}$ (%)	References
1	Camargue silt	36	600	19	17	This study
2	Sikkak clay	50	1000	18	32	
3	Châtaignier clay	71	2500	24	47	
4	Maghnia clay	112	3000	26	86	
5	Sterrebeek loam	27	26	22	5	Zerhouni [91]
6	Vieuxpré clay	32	800	19	13	Indarto [45]
7	Red mari	36	500	16	20	Biarez et al. [14]
8	Jossigny loam	37	800	15	22	Indarto [45]
9	Yellow clay	40	700	22	18	Indarto [45]
10	Gault clay	42	800	18	24	Croney and Cloeman [27]
11	Bouhennak marl	47	1000	14	33	Benchouk [12]
12	St. Rosalie clay	48	700	24	24	Yong et al. [90]
13	Scott clay	49	2000	16	33	Blight [18]
14	Mers El Kebir clay	49	1500	24	25	Bourokba et al. [19]
15	Boughrara clay	54	2000	13	41	Derfouf et al. [29]
16	Silt	55	800	25	30	Fredlund [36]
17	London clay	78	2500	25	53	Croney and Cloeman [27]
18	Kaolin	80	2000	40	40	Yong et al. [90]
19	Maghnia Bentonite	130	3000	20	110	Benchouk [12]
20	Allophane	140	4500	45	95	Hagiwara et al. [43]
21	Montmorillonite	170	4500	25	145	Fleureau et al. [32]
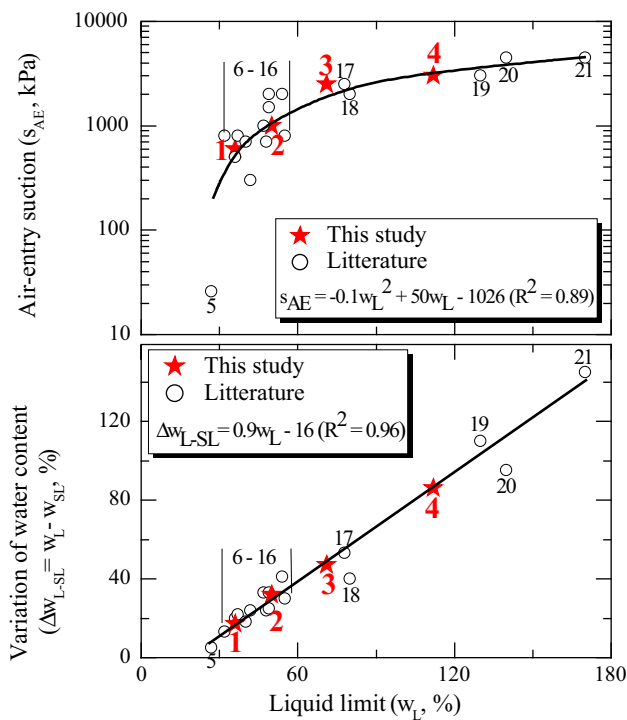
Fig. 12 Correlation between air-entry suction and the change in water content with liquid limit

$$e = G_s/\rho_d - 1$$
$$S_r = wG_s/e = wG_s/(G_s/\rho_d - 1)$$

Figure 15 presents the global representation of compaction curves at standard Proctor compaction energy and of the drying–wetting curves. Even though with different results on a different soil, our observation is similar to that of Fleureau et al. [35]. In the air-occlusion zone that corresponds to the wet side of the optimum ($w > w_{opt}$), the compaction curve is very close to the wetting curve. In this regard, it is possible to derive the wetting curve of the compacted soil from the measurements of suction after compaction at different water contents larger than the optimum. Below the air-occlusion zone ($w < w_{opt}$), the compaction path is located below the drying curve as a result of the presence of a large quantity of air bubbles. To highlight such difference, it is necessary to understand the nature of compaction and drying–wetting curves:

- the compaction curve describes the final state of soil samples after a mechanical process during which the air phase is compressed or driven out at different initial water contents. Generally, the line representing this

Table 3 Materials used for the correlation of standard Proctor optimum water content (w_{SPO}), suction (s_{SPO}), dry density ($\rho_{d\text{-}SPO}$), swelling indices with respect to void ratio (C_{ms}), swelling index with respect to water content (D_{ms})

Material no.	Soil	w_L (%)	w_{SPO} (%)	s_{SPO} (%)	$\rho_{d\text{-}SPO}$ (g/cm3)	C_{ms}	D_{ms}	References
1	Camargue silt	36	17.2	100	1.72	−0.067	−3.3	This study
2	Sikkak clay	50	16	600	1.55	−0.15	−5.5	
3	Châtaignier clay	71	37.5	800	1.31	−0.13	−6.3	
4	Maghnia clay	112	18	3500	1.23	−0.5	−17.5	
5	21 soils	17–90	9.8–32.5	30–3399	1.30–1.94	(−0.006, −0.04)	(−0.4, −3.2)	Fleureau et al. [35]
6	20 soils	34–103	17.1–40.9	–	1.22–1.91	–	–	Kheirbek Saoud [47]
7	La verne	35	16.5	20	1.79	−0.05[a]	–	Taibi et al. [77]
8	Silty clay 90P300/5RF/ 5S	38	18	650	1.67	−0.11[a]	−4.5[a]	Sayad-Gaidi [75]
9	Boughrara marl	48	21	620	1.62	−0.16[a]	−7.2[a]	Taibi et al. [77]
10	Sikkak marl	50	16	1032	1.55	−0.15[a]	−7.5[a]	Taibi et al. [77]
11	Boughrara clay	54	21	990	1.62	–	–	Derfoufet al. [30]

[a] Estimated
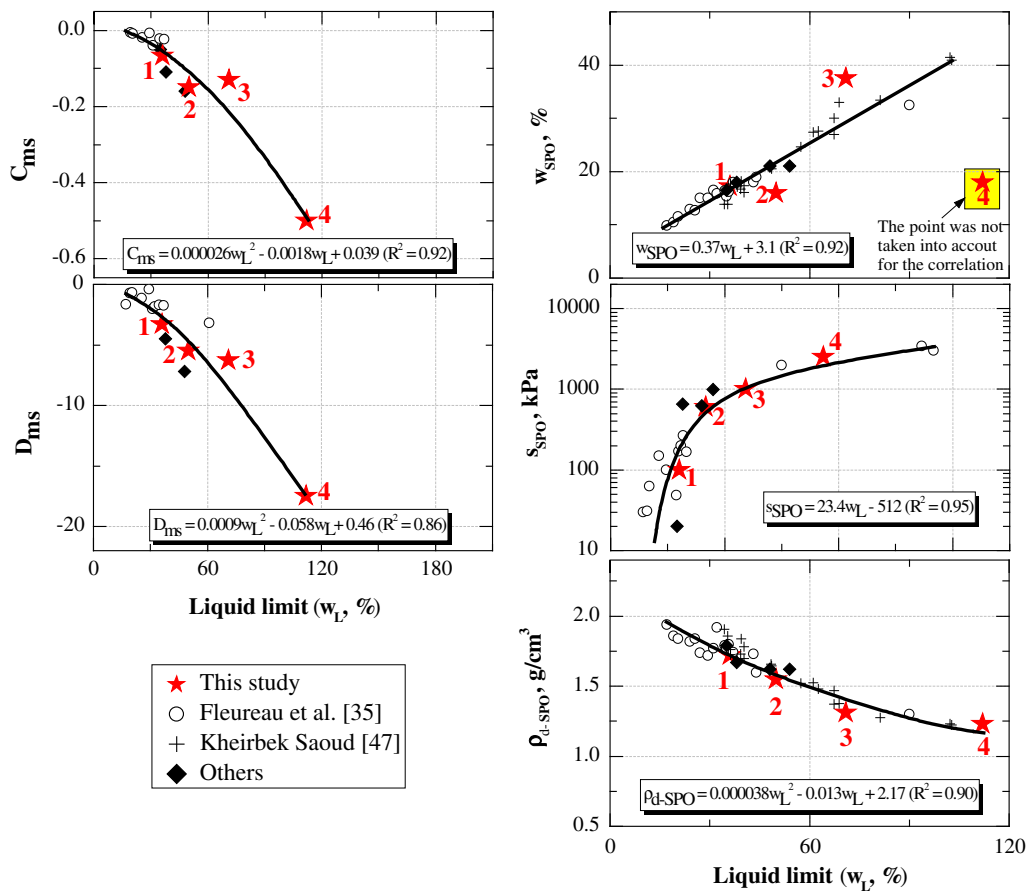
Fig. 13 Correlation between standard Proctor optimum water content (w_{SPO}), maximum dry density ($\rho_{d\text{-}SPO}$), suction at the optimum water content (s_{SPO}), swelling index with respect to void ratio(C_{ms}),swelling index with respect to water content (D_{ms}) and liquid limit
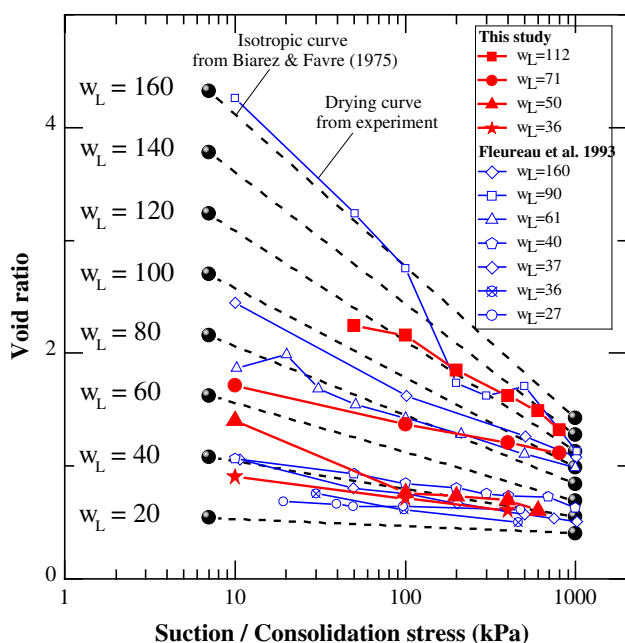
Fig. 14 Representation of experimental drying curves for the soils of this study and several others from Fleureau et al. [33] in the void ratio versus suction diagram

mechanical process is vertical in the (S_r, w) diagram as water content can be considered as constant.

- the drying–wetting curves describe the final state of samples compacted at a selected water content after a hydraulic process in which water is transferred from samples to the environment or inversely. The hydraulic process can be represented by the inclined dotted lines in Fig. 15.

More specifically, in the (w, s) plane, the compaction curve is consistent with the drying–wetting curves, especially on the wet side of the optimum.

7.3 Comparison of the water retention curves obtained by different methods

In this study, water retention curves were determined using three approaches: direct measurement of suction and water content in compaction test; measurement of water content under controlled suction conditions during drying–wetting tests; and calculation of the equivalent suction and water content from MIP test.

As shown in Fig. 16, for the direct measurement of suction, the two methods, filter-paper and psychrometer, show an excellent consistency in spite of the relatively limited number of experimental data; as regards suction control, the experimental results of DVS are in very good agreement with those of the desiccator; comparing the WRC from suction measurement and suction control, the results are satisfactory, even though there are some

differences for suctions smaller than 1000 kPa, probably due to (1) the metamorphism of the filter-paper (presence of mould) under high water content conditions; (2) the fact that the tensiometric plate and osmotic methods measure matrix suction, whereas the psychrometer measures total suction.

Previous works (e.g. [28, 54, 62, 65, 69]) suggested the possibility to derive the water retention curve from MIP test. Assuming that the mercury intrusion process, in which the non-wetting liquid (mercury) penetrating the porous medium full of a wetting fluid (mercury vapour under vacuum) is equivalent to the drying path in which the wetting liquid (water) moves out of soil. The equivalent suction and water content can be calculated as follows:

$$s = -\frac{T_w \cos\theta_w}{T_{Hg} \cos\theta_{Hg}} p_{Hg} = 0.196 p_{Hg}$$

$$w = V_{mercury} / m_s$$

in which s is the suction corresponding to the mercury intrusion pressure (p_{Hg}); T_w, T_{Hg} represent the surface tensions of water and mercury, respectively (at 20 °C, $T_w = 72.75 \times 10^{-3}$ N/m for air–water interface and $T_{Hg} = 485 \times 10^{-3}$ N/m for liquid mercury–mercury vapour interface); θ_w and θ_{Hg} are the contact angles of water–solid and mercury–solid phases ($\theta_w = 0°$ and $\theta_{Hg} = 140°$); w, $V_{mercury}$ and m_s represent the equivalent water content, intruded mercury volume and solid mass, respectively.

Figure 16 shows the comparison between the water retention curve (WRC) derived from the MIP test and that derived from drying–wetting tests. In general, there is a similar shape for the two WRC curves, but that determined by MIP test (empty circle line) is located on the left side of that of the drying–wetting experiments.

However, according to some authors (Cui [28], Romero [69]), if a residual water content (e.g. 10% for the very plastic Châtaignier clay) is taken into account, the modified results (solid circle line) are reasonably close to the experimental data, especially for suctions larger than 3 MPa. Considering the high plasticity of the Châtaignier clay and the high percentage of non-accessible pores by mercury, such results are reasonable and acceptable.

8 Conclusion

The tests that were presented in this paper were initially intended to show the interest of the global representation of the drying–wetting curves of different engineering soils. Such representation allows particularly monitoring the saturation of the soil, linking swelling–shrinkage characteristics with suction, etc. Several interesting and useful features have been emphasized.
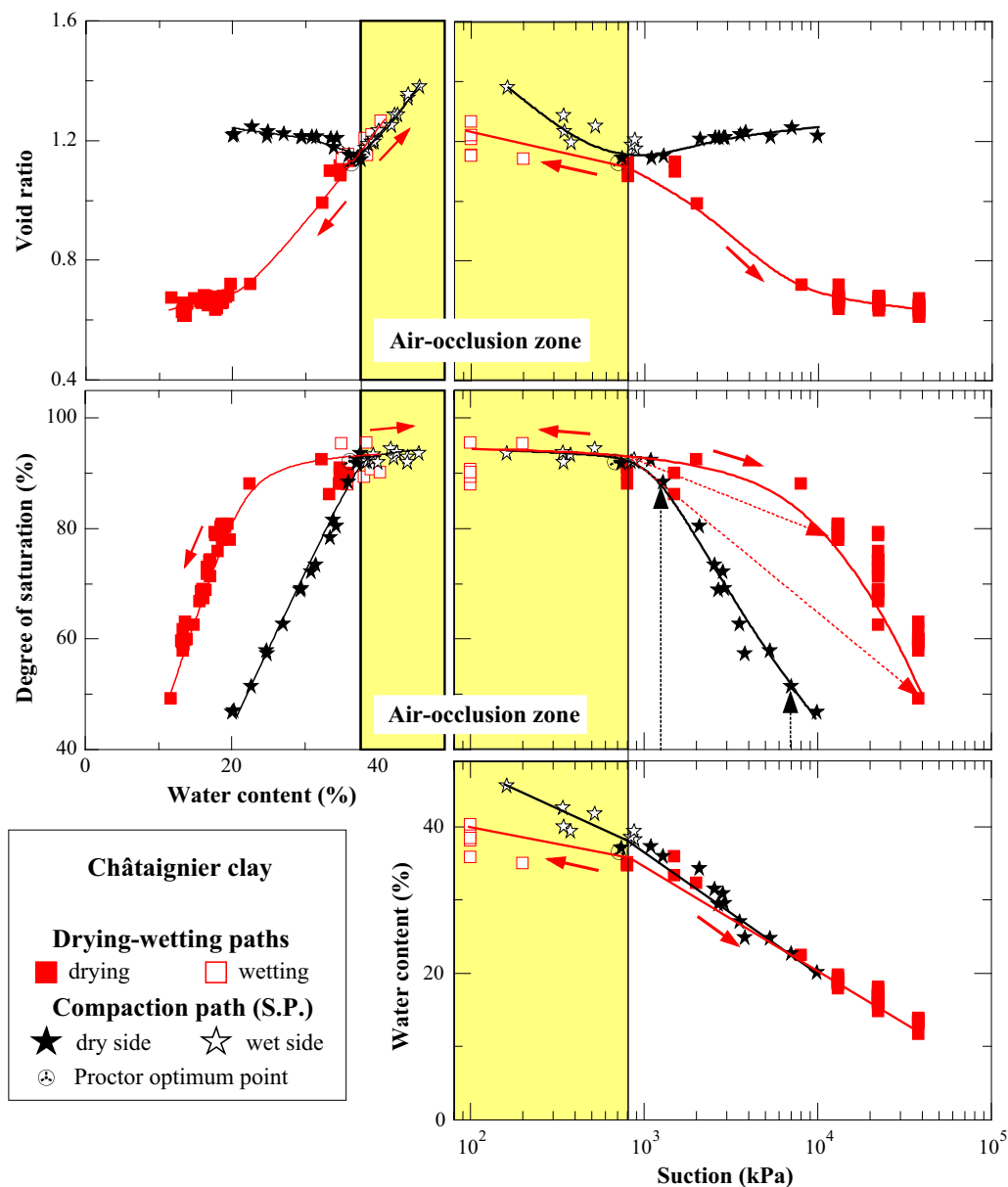
Fig. 15 Analogy between compaction and drying–wetting curves (standard Proctor)

Concerning the drying–wetting curves of the saturated slurries:

- hysteresis is apparent in the plane of void ratio or saturation versus suction, and it almost disappears when plotting the parameters against water content;
- as the representative parameter of soil nature, liquid limit has an essential influence on the characteristics of the drying–wetting curves of slurries or samples compacted under standardized conditions, in particular the air-entry suction and shrinkage limit water content;
- the mechanical stress (oedometric or isotropic loading) and suction have an equivalent effect in terms of volume change in the quasi-saturated domain, showing

the validity of the Terzaghi effective stress for saturated soils under suction; the empirical correlations of Biarez and Favre [13] were shown to provide a fairly good first estimation of drying curve.

As regards the drying–wetting curves of the compacted samples:

- from a microscopic point of view, suction has a significant influence on the inter-aggregate pores and a suction large enough may lead to the closing of the inter-aggregate pores, whereas the intra-aggregate pores are not influenced in the case of the studied soil and applied suctions;
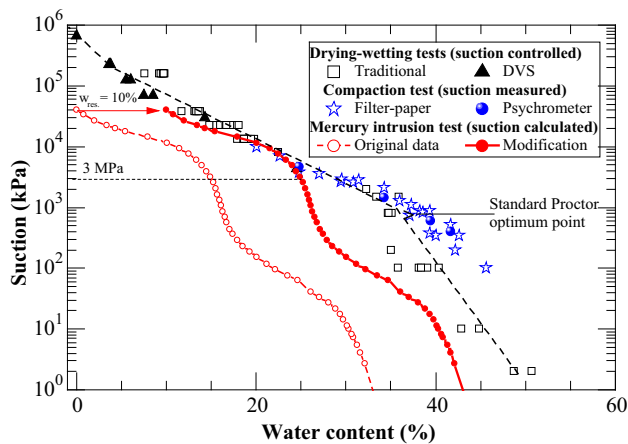
Fig. 16 Determination of the water retention curve (WRC) from suction control, suction measurement and mercury intrusion porosimetry (MIP) tests ("Traditional" means the tensiometric plate, osmotic and desiccator methods; DVS represents the dynamic vapour sorption method; to transfer the original data to the modification, a quantity of 10% of the residual water content was added to the original data of the MIP test)

- the initial compaction water content influences the air-entry suction and the soil sample prepared on the dry side of the optimum has a smaller air-entry suction, whereas, for the studied soil (Châtaignier clay) and the applied energies (0.36, 0.60 and 0.84 MJ/m^3), the influence of energy on the drying–wetting curves is negligible.

In addition, the comparison between the different curves highlighted several interesting observations:

- even though very different mechanisms are involved, the compaction curve is close to the wetting curve in the air-occlusion zone corresponding to the wet side of the Proctor optimum; therefore, it is possible to determine the wetting curve from the suctions measured after Proctor compaction tests;
- the different methods of controlling and measuring suction showed a reasonable agreement in the determination of the water retention curve; the water retention curve determined from the pore size distribution curve proved consistent with the drying curve for suctions higher than 3 MPa.

Finally, correlations between different characteristic parameters of drying–wetting curves were established. Satisfactory results were obtained using the liquid limit to model the drying–wetting curves, without excluding other intrinsic parameters for further comprehensive modelling.

References

1. AFNOR (1991) Sols: reconnaissance et essais - Détermination de la masse volumique des particules solides des sols - Méthode du pycnomètre à eau, AFNOR NF P94-054. AFNOR Group, France
2. AFNOR (1992) Sols: reconnaissance et essais - Analyse granulometrique des sols - Méthode par sédimentation, AFNOR NF P94-057. AFNOR Group, France
3. AFNOR (1996) Sols: reconnaissance et essais - Analyse granulométrique - Méthode par tamisage à sec après lavage. AFNOR NF P94-056. AFNOR Group, France
4. AFNOR (1993) Sols: reconnaissance et essais - Détermination des limites d'Atterberg - Limite de liquidité à la coupelle - Limite de plasticité au rouleau, AFNOR NF P94-051. AFNOR Group, France
5. AFNOR (2014) Sols: reconnaissance et essais - Détermination des références de compactage d'un matériau - Essai Proctor normal - Essai Proctor Modifié. AFNOR NF P94-093. AFNOR Group, France
6. Alonso EE, Gens A, Josa A (1990) A constitutive model for partially saturated soils. Géotechnique 40(3):405–430
7. Alonso EE, Romero E, Hoffmann C, García-Escudero E (2005) Expansive bentonite-sand mixtures in cyclic controlled-suction drying and wetting. Eng Geol 81(3):213–226
8. Alonso EE, Pereira JM, Vaunat J, Olivella S (2010) A microstructurally based effective stress for unsaturated soils. Géotechnique 60(12):913–925
9. Alonso EE, Pinyol NM, Gens A (2013) Compacted soil behaviour: initial state, structure and constitutive modelling. Géotechnique 63(6):463–478
10. ASTMD 6836-02 (2003) Standard test method for determination of the soil water characteristic curve for desorption using a hanging column, pressure extractor, chilled mirror hygrometer, and/or centrifuge. Annual book of ASTM standards. Section 4: soil and rock, vol 04.08. American Society for Testing Materials, West Conshohocken
11. Benchouk A, Derfouf M, Abou-Bekr N, Taibi S (2012) Behaviour of some clays on drying and wetting paths. Arab J Geosci 6(12):4565–4573
12. Benchouk A (2014) Comportement hydromécanique des sols fins compactés au voisinage de la saturation. Doctoral dissertation, Université Abou-Bekr Belkaid de Tlemcen, Algeria
13. Biarez J, Favre JL (1975) Parameters filling and statistical analysis of data in soil mechanics. In: Proceedings of 2nd international conference on applications of statistics and probability in soil mechanics, Aachen 2, pp 249–264
14. Biarez J, Fleureau JM, Zerhouni MI, Soepandji BS (1987) Variations de volume des sols argileux lors de cycles de drainage-humidification. Rev Fr Géotech 41:63–71
15. Biarez J, Fleureau JM, Taibi S (1994) Critère de résistance maximale des sols non saturés: Approche expérimentale et modélisation. In: Proceedings of the 13th International Conference on Soil Mechanics and Foundation Engineering, New-Delhi, January, Oxford & I.B.H. Pub. co., pp 385–388
16. Black WPM (1962) A method of estimating the California bearing ratio of cohesive soils from plasticity data. Géotechnique 12(4):271–282
17. Blatz JA, Cui YJ, Oldecop L (2008) Vapour equilibrium and osmotic technique for suction control. Geotech Geol Eng 26(6):661–673
18. Blight GE (1966) Strength characteristics of desiccated clays. J Soil Mech Found Div 92(6):18–38
19. Bourokba MS, Hachichi A, Fleureau JM (2007) Comportement de l'argile de Mers El Kebir sur chemin d'humidification drainage. Colloque sols et matériaux à problèmes.9-11 Février, Tunis

20. Buckingham E (1907) Studies on the movement of soil moisture. U. S. Department of Agriculture Bureau of Soils-Bulletin No. 38, p 64
21. Bulut R, Lytton RL, Wray WK (2001) Soil suction measurements by filter paper. In: Vipulanandan C, Addison MB, Hasen M (eds) Expansive clay soils and vegetative influence on shallow foundations. ASCE geotechnical special publication no. 115, Houston, Texas, pp 243–261
22. Casagrande A (1948) Classification and identification of soils. Trans Am Soc Civil Eng 113(1):901–930
23. Chandler RJ, Crilly MS, Smith MG (1992) A low-cost method of assessing clay desiccation for low-rise buildings. Proc Inst Civil Eng Civil Eng 92(2):82–89
24. Cnudde V, Boone MN (2013) High-resolution X-ray computed tomography in geosciences: a review of the current technology and applications. Earth Sci Rev 123:1–17
25. Coronado O, Caicedo B, Taibi S, Correia AG, Fleureau JM (2011) A macro geomechanical approach to rank non-standard unbound granular materials for pavements. Eng Geol 119(1):64–73
26. Croney D (1952) The movement and distribution of water in soils. Géotechnique 3(1):1–16
27. Croney D, Coleman JD (1954) Soil structure in relation to soil suction. J Soil Sci 5:75–84
28. Cui YJ (1993) Etude du comportement d'un limon compacté non saturé, et de sa modélisation dans un cadre élasto-plastique. Doctoral dissertation, Ecole Nationale des Ponts et Chaussées, France
29. Derfouf FEM, Allal MA, Abou-Bekr N, Taibi S (2013) Mesure et prédiction des chemins de drainage humidification. Application à l'argile d'un noyau de barrage. Rev Fr Géotech 142:49–60
30. Derfouf FEM (2014) Contribution à l'étude des sols fins non saturés: Aspects du comportement volumique. Doctoral dissertation, Université Abou-Bekr Belkaid de Tlemcen, Algeria
31. Delage P, Marcial D, Cui YJ, Ruiz X (2006) Ageing effects in a compacted bentonite: a microstructure approach. Géotechnique 56(5):291–304
32. Fleureau JM, Soemitro R, Taibi S (1992) Behaviour of an expansive clay related to suction. In: Proceedings 7th international conference on expansive soils, Dallas, vol 1, pp 173–178
33. Fleureau JM, Kheirbek-Saoud S, Soemitro R, Taibi S (1993) Behaviour of clayey soils on drying–wetting paths. Can Geotech J 30(2):287–296
34. Fleureau JM, Kheirbek-Saoud S (2001) Retrait et Gonflement des sols soumis à un cycle de drainage humidification. Colloque international «Génie Civil et Constructions», Université de Damas, Syrie, 1–3 Octobre
35. Fleureau JM, Verbrugge JC, Huergo PJ, Correia AG, Kheirbek-Saoud S (2002) Aspects of the behaviour of compacted clayey soils on drying and wetting paths. Can Geotech J 39(6):1341–1357
36. Fredlund DG (1967) Comparison of soil suction and one-dimensional consolidation characteristics of a highly plastic clay. National Research Council of Canada, Division of Building Research, Technical Paper 245
37. Fredlund DG, Xing A, Huang S (1994) Predicting the permeability function for unsaturated soils using the soil-water characteristic. Can Geotech J 31(4):533–546
38. Fredlund DG, Xing A, Fredlund MD, Barbour SL (1996) The relationship of the unsaturated shear strength function to the soil-water characteristic. Can Geotech J 33(3):440–448
39. Gardner W, Israelsen O, Edlefsen N, Clyde D (1922) The capillary potential function and its relation to irrigation practice. Phys Rev 20(2):196–205
40. Geremew Z, Audiguier M, Cojean R (2009) Analyse du comportement d'un sol argileux sous sollicitations hydriques cycliques. Bull Eng Geol Environ 68(3):421–436
41. Ghembaza MS, Taibi S, Fleureau JM (2007) Effet de la température sur le comportement des sols non saturés sur les chemins de drainage et d'humidification. Can Geotech J 44(9):1064–1081
42. Gupta S, Larson WE (1979) Estimating soil water retention characteristics from particle size distribution, organic matter percent and bulk density. Water Resour Res 15(6):1633–1635
43. Hagiwara M, Takenaka H (1985) Shrinkage and structure of allophane soil. Soils Found 25(2):77–85
44. Ho DYF, Fredlund DG, Rahardjo H (1992) Volume change indices during loading and unloading of an unsaturated soil. Can Geotech J 29(2):195–207
45. Indarto (1991) Comportement des sols soumis à une pression interstitielle négative: application aux silos. Doctoral dissertation, École Centrale Paris, France
46. Jennings JE (1961) A revised effective stress law for use in the prediction of the behaviour of unsaturated soils. In: Conference on pore pressure and suction in soils (British National Society of Soil Mechanics). Butterworth, London, pp 26–30
47. Kheirbek Saoud S (1994) Comportement mécanique de le couche de foundation d'une voie ferrée. Doctoral dissertation, École Centrale Paris, France
48. Kohgo Y, Nakano M, Miyazaki T (1993) Theoretical aspects of constitutive modelling for unsaturated soils. Soils Found 33(4):49–63
49. Kohgo Y, Nakano M, Miyazaki T (1993) Verification of the generalized elastoplastic model for unsaturated soils. Soils Found 33(4):64–73
50. Kohgo Y (2002) Elastoplastic models for unsaturated soils with two suction effects and unsaturated soil behaviour. In: Proceedings of the 3rd international conference on unsaturated soils. Swets & Zeitlinger, Lisse, pp 905–915
51. Laloui L, Salager S, Rizzi M (2013) Retention behaviour of natural clayey materials at different temperatures. Acta Geotech 8(5):537–546
52. Li ZM (1995) Compressibility and collapsibility of compacted unsaturated loessial soils. In: Proceeding of the 1st international conference on unsaturated soils, Paris, vol 1, pp 139–144
53. Li ZS (2015) Etudes des propriétés hydromécaniques des sols argileux non saturés proches de la saturation. Doctoral dissertation, Ecole Centrale Paris, France
54. Liu XF, Buzzi O, Yuan S, Mendes J, Fityus S (2016) Multi-scale characterization of the retention and shrinkage behaviour of four Australian clayey soils. Can Geotech J 53(5):854–870
55. Lloret A, Alonso EE (1985) State surfaces for partially saturated soils. In: Proceedings of the 11th international conference on soil mechanics and foundation engineering, San Francisco, vol 2, pp 557–562
56. Lu N, Likos WJ (2006) Suction stress characteristic curve for unsaturated soil. J Geotech Geoenviron Eng 132(2):131–142
57. Marinho FAM (1994) Shrinkage behaviour of some plastic soils. Doctoral dissertation, University of London, UK
58. Marinho FAM, Stuermer M (2000) The influence of the compaction energy on the SWCC of a residual soil. Advances in unsaturated geotechnics. ASCE geotechnical special publication, Colorado, Denver, USA, pp 125–141
59. Marinho FAM (2005) Nature of soil-water characteristic curve for plastic soils. J Geotech Geoenviron Eng 131(5):654–661
60. Marinho FAM (2006) A method of estimating the soil-water retention curve for plastic soils. In: Miller GA, Zapata CE, Houston SL, Fredlund DG (eds) Fourth international conference on unsaturated soils, Carefree (Arizona). ASCE, pp 1473–1481
61. Modaressi A, Abou-Bekr N, Fry JJ (1996) Unified approach to model partially saturated and saturated soils. In: Proceeding of the 1st international conference on unsaturated soils, Paris, vol 3, pp 111–116

62. Muñoz-Castelblanco JA, Pereira JM, Delage P, Cui YJ (2012) The water retention properties of a natural unsaturated loess from northern France. Géotechnique 62(2):95–106

63. Nanda A, Delage P, Nedjat N, Fry JJ, Gatmiri B (1993) Evaluation de la sécurité des remblais en cours de construction: le code UDAM. Rev Fr Géotech 62:23–34

64. Ng CWW, Pang YW (2000) Influence of stress state on soil-water characteristics and slope stability. J Geotech Geoenviron Eng 126(2):157–166

65. Prapaharan S, Altschaeffl AG, Dempsey BJ (1985) Moisture curve of compacted clay-mercury intrusion method. J Geotech Eng ASCE 111(9):1139–1146

66. Richards LA (1941) A pressure-membrane extraction apparatus for soil solution. Soil Sci 51(5):377–386

67. Richards LA (1942) Soil moisture tensiometer materials and construction. Soil Sci 53(4):241–248

68. Richards LA (1949) Methods of measuring soil moisture tension. Soil Sci 68(1):95–112

69. Romero E (1999) Characterization and thermo-hydro-mechanical behaviour of unsaturated Boom clay: an experimental study. Doctoral dissertation, Universitat Politècnica de Catalunya, Spain

70. Romero E, Gens A, Lloret A (1999) Water permeability, water retention and microstructure of unsaturated compacted Boom clay. Eng Geol 54(1):117–127

71. Romero E, Simms PH (2008) Microstructure investigation in unsaturated soils: a review with special attention to contribution of mercury intrusion porosimetry and environmental scanning electron microscopy. Geotech Geol Eng 6(26):705–727

72. Romero E, Della Vecchia G, Jommi C (2011) An insight into the water retention properties of compacted clayey soils. Géotechnique 61(4):313–328

73. Romero E (2013) A microstructural insight into compacted clayey soils and their hydraulic properties. Eng Geol 165:3–19

74. Salager S, Rizzi M, Laloui L (2011) An innovative device for determining the soil water retention curve under high suction at different temperatures. Acta Geotech 6(3):135–142

75. Sayad-Gaidi S (2003) Ecoulements dans les milieux poreux peu perméables saturés et non saturés. Doctoral dissertation. Université du Havre, France

76. Taibi S (1994). Comportement mécanique et hydraulique des sols soumis à une pression interstitielle négative - etude expérimentale et modélisation. Doctoral dissertation. Ecole Centrale Paris, France

77. Taibi S, Fleureau JM, Abou-Bekr N, Zerhouni MI, Benchouk A, Lachgueur K, Souli H (2011) Some aspects of the behaviour of compacted soils along wetting paths. Géotechnique 61(5):431–437

78. Tarantino A, De Col E (2008) Compaction behaviour of clay. Géotechnique 58(3):199–213

79. Terzaghi K, Peck RB (1967) Soil mechanics in engineering practice, 2nd edn. Wiley, New York

80. Tripathy S, Tadza MYM, Thomas HR (2014) Soil-water characteristic curves of clays. Can Geotech J 51(8):869–883

81. Van Genuchten MT (1980) A closed form equation predicting the hydraulic conductivity of unsaturated soils. Soil Sci Soc Am J Impact 44:892–898

82. Vanapalli SK, Fredlund DG, Pufahl DE (1999) The influence of soil structure and stress history on the soil-water characteristics of a compacted till. Géotechnica 49(2):143–159

83. Vanapalli SK, Nicotera MV, Sharma RS (2008) Axis translation and negative water column techniques for suction control. Geotech Geol Eng 26(6):645–660

84. Verbrugge JC (1974) Contribution à la mesure de la succion et de la pression interstitielle dans les sols non saturés. Doctoral dissertation, Université Libre de Bruxelles, Belgium

85. Verbrugge JC (1978) Emploi d'une méthode psychrométrique dans des essais triaxiaux sur un limon remanié non saturé. Revue Canadienne de Géotechnique 15(5): 501–509, and 1979 Discussion 16(3): 615–616

86. Verbrugge JC, Fleureau JM (2002) Bases expérimentales du comportement des sols non saturés. Coussy O, Fleureau JM (eds) Mécanique des sols non saturés Coll. MIM. Hermès, Paris, pp 69–112

87. Vincent M (2003) Retrait-gonflement des sols argileux: méthode cartographique d'évaluation de l'aléa en vue de l'établissement de PPR. 3ème conférence SIRNAT-Forum des journées pour la Prévention des Risques Naturels, Orléans, janv. 2003

88. Wei X, Hattab M, Fleureau JM, Hu R (2013) Micro-macro-experimental study of two clayey materials on drying paths. Bull Eng Geol Environ 72(3–4):495–508

89. Wheeler SJ, Karube D (1996) Constitutive modelling. In: Proceeding of the 1st international conference on unsaturated soils, Paris, vol 3, pp 1323–1356

90. Yong RN, Warkentin BP (1975) Soil properties and behaviour, development in geotechnical engineering series, Chap. 4. Elsevier, Amsterdam, p 4

91. Zerhouni MI (1991) Rôle de la pression interstitielle negative dans le comportement des sols-Application au calcul des routes, Doctoral dissertation, Ecole Centrale Paris, France